

Astrophysics in the heliosphere: interplanetary medium, Sun-Earth coupling and cosmic rays transport

S. Dasso^{1,2}

¹ *Instituto de Astronomía y Física del Espacio, CONICET-UBA, Argentina*

² *Departamento de Ciencias de la Atmósfera y los Océanos, FCEN-UBA, Argentina*

Contact / sdasso@iafe.uba.ar

Resumen / La heliosfera presenta una gran riqueza y variedad de procesos dinámicos, tales como turbulencia magnetohidrodinámica (MHD), reconexión magnética, relajación a estados lineales libres de fuerzas (i.e., estados de Taylor), inestabilidades en plasmas, difusión y derivas de rayos cósmicos, entre otros. La accesibilidad a observaciones *in situ* de propiedades físicas asociadas con estos procesos convierten a la heliosfera en un sistema único para mejorar nuestro conocimiento y elaborar modelos más avanzados sobre procesos astrofísicos universales que también están presentes en otras escalas y otros objetos fuera de nuestro sistema solar. El medio interplanetario que compone la heliosfera presenta diferentes fases dependiendo tanto de la actividad solar que origina el plasma, el campo magnético y las partículas energéticas que lo componen, como de su evolución a medida que se propaga hacia el medio interestelar local. A lo largo de este trabajo se presentará una revisión de las propiedades principales del medio interplanetario y una puesta al día del conocimiento de los procesos principales que ocurren durante la evolución dinámica de los eventos transitorios más relevantes, denominados *Interplanetary Coronal Mass Ejections* (ICMEs), así como también su vínculo con el acoplamiento Sol-Tierra y con el transporte de rayos cósmicos galácticos.

Abstract / The heliosphere presents a huge richness and variety of dynamical processes, such as MagnetoHydrodynamical (MHD) turbulence, magnetic reconnection, relaxation toward linear force free MHD states (i.e., Taylor states), plasma instabilities, diffusion and drift of cosmic rays, among other processes. The accessibility to *in situ* observations of different physical properties associated with these processes makes it a unique system to improve our knowledge and develop more advanced models of universal astrophysical processes that are also present at other scales and objects outside of our solar system. The interplanetary medium that makes up the heliosphere presents different phases, depending on the solar activity that originates the plasma, the magnetic field and the energetic particles that compose it, and on its evolution over time, as it propagates out into the local interstellar medium. The objective of this work is to present a review and the state of the art about the main properties of the interplanetary medium. In particular, about the main physical processes happening during the dynamic evolution of major transient solar events (called *Interplanetary Coronal Mass Ejections*, ICMEs) when they travel towards the Earth, as well as about their link with the Sun-Earth coupling and with the galactic cosmic rays transport.

Keywords / Sun: heliosphere — solar wind — interplanetary medium — solar-terrestrial relations — cosmic rays

1. Introduction

The solar variability determines the interplanetary plasma and magnetic properties of the heliosphere (i.e., the solar system's magnetic cavity, including the space environment of planets and satellites). Different time/space scales are involved in different solar and interplanetary physical processes, from milliseconds to thousands of years and from the gyro-cycle radius of ions/electrons to the size of the entire solar system. Solar activity can severely affect space and atmospheric planetary conditions, such as solar radiative flux, energetic particles coming from the Sun, variability of the solar wind plasma conditions, and interplanetary transients.

In particular, the interplanetary manifestation of transient solar ejections, called Interplanetary Coronal Mass Ejections (ICMEs), are one of the most important events at time scales of about hours or days and space scales from the solar radius to ~ 0.1 au (e.g., Dasso

et al., 2005b). These solar-interplanetary transients can affect the Sun-Earth coupling level, seriously affecting the geo-space and driving disturbances into the terrestrial magnetosphere and atmosphere. An extra motivation for understanding them at a deeper level is to forecast them, because the ICMEs have some social implications. In particular, some extreme events can negatively affect different modern technology infrastructures in space and on the ground, such as spacecraft losses or large-scale electric power blackouts, (e.g., Baker et al., 2013; Hayakawa et al., 2019; Hapgood et al., 2022).

The Scientific Committee on Solar-Terrestrial Physics (SCOSTEP), which is a thematic body of the International Science Council (ISC), defined its next scientific program as PREDictability of the variable Solar-Terrestrial cOupling (PRESTO). The present paper will focus on ICMEs and galactic cosmic rays (GCRs) which belong to the core of the key milestones of the PRESTO roadmap for the next 5 years, from 2020 to 2024 (Daglis et al., 2021), and are major and key topics inside Divi-

sion E (Sun and Heliosphere) of the International Astronomical Union.

The paper starts describing large scale (stationary and transient) properties of the interplanetary medium, and also their fluctuations (Section 2). The main physical effects that occur during the transport of GCRs in the solar wind are presented (Section 3). Then, in Section 4, the first Space Weather laboratory located in an Argentine Antarctic base, containing a GCRs detector, is introduced. Finally, the summary and conclusions of this manuscript can be found in Section 5.

2. The interplanetary medium

The solar plasma outflows are a natural consequence of the solar corona high temperature. The pressure is much larger at the solar corona than at the outer part of the heliosphere. The pressure gradient wins gravity and originates the super-critical solar wind, transporting solar material to the local interstellar medium with the parcels of magneto-fluid travelling almost radially from the Sun.

2.1. The Parker spiral

The interplanetary plasma at large and mesoscales can be modelled using magnetohydrodynamics (MHD). Particularly, many of the plasma regimes can be described in the framework of an almost ideal MHD (i.e., very low magnetic resistivity). This implies that MHD invariants, such as magnetic flux/helicity are almost preserved. The configuration of the Interplanetary Magnetic Field (IMF) raises from the solar rotation and conservation of the IMF flux, and the consequent frozen-in flux (e.g., Russell et al., 2016), forming the so-called Parker spiral, similar to the water spiral created by a garden sprinkler. At the ecliptic plane and at a given heliodistance D (i.e., distance from the Sun), the angle (α), formed between the radial from the Sun and the projection of the IMF vector on the ecliptic plane, can be theoretically estimated as $\tan(\alpha) = B_\phi/B_r = \frac{\Omega D}{V_{sw}}$, where B_ϕ and B_r are the azimuthal (on ecliptic plane) and radial (from the Sun) components of the IMF, Ω is the angular velocity of the solar rotation, and V_{sw} is the solar wind bulk velocity, which is mainly radial. For a value of $V_{sw} \sim 400$ km/s, a Parkerian IMF at 1 au is expected to have a direction such as $\alpha \sim 45^\circ$ for a magnetic sector out-going from the Sun (and $\alpha \sim -135^\circ$ for a magnetic sector toward the Sun).

Figure 1 shows α in two different periods of time where the solar wind was characterized as Parkerian (i.e., not disturbed with transient structures, see later in this section). Interplanetary data shown in all figures of this paper were observed from plasma measurements obtained from SWEPAM and MAG instruments aboard the Advanced Composition Explorer (ACE) satellite, which is located at the Lagrange point L1.

Two periods of 6 hours are shown: (a) the upper panel shows data observed (green dots) on June 10, 2002 (from 7 to 13 UT), where $\alpha \sim -135^\circ$, it corresponds to a magnetic sector going towards the Sun; (b) the bot-

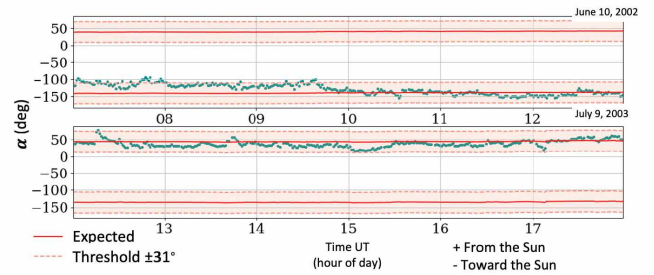


Figure 1: Observations at 1 au of parkerian IMF: (a) *upper panel* where the IMF was in-ward, and (b) *bottom* where the IMF was out-ward to the Sun.

tom panel shows data observed (green dots) on July 9, 2003 (from 12 to 18 UT), where $\alpha \sim 45^\circ$, it corresponds to a magnetic sector coming out of the Sun. The solid red lines represent the two (inward/outward polarities) expected values of α for a Parker IMF, and the red-shadowed area and dashed red lines correspond to its statistical threshold (for more details see Dorsch et al. (2022)). An operative tool presenting the α angle in real time is available at the website of LAMP (Laboratorio Argentino de Meteorología del espacio: spaceweather.at.fcen.uba.ar). For more details of operative products and activities developed by the LAMP Space Weather laboratory, see Lanabere et al. (2020b) and Lanabere et al. (2021).

2.2. Transient solar wind structures

The Sun's surface presents dark regions in the range of extreme ultra-violet and x-rays, called coronal holes (CHs). CHs were originally recognized as low-density regions and as typical sources of fast solar wind. The activity of the Sun follows a ~ 11 years solar cycle. While the magnetic configuration in the solar atmosphere is mostly nearly dipolar with CHs located around the poles and slowly varying during a solar minimum, in a solar maximum, the corona shows streamer structures and CHs can be found over a wide range of solar latitudes.

From a similar point of view as in section 2.1, and due to the solar rotation, the solar source region of the solar wind provides interplanetary material to different angular sectors. When, at a given solar wind cone, the material was slowly provided in the first place and then a CH provides it in a faster way, a stream interaction region is formed.

These structures, called stream interaction regions (SIRs), evolve with D and are one of the most important transient structures in the interplanetary (IP) medium, deforming the IMF spiral and, sometimes, producing compression regions (where the fast material reaches the slow fluid) and interplanetary shock waves when the relative velocities are super critical (larger than the active wave modes of the system). When a CH lives more than a solar rotation period, SIRs can be observed repeatedly once every ~ 27 days, and then they are known as co-rotating interaction regions (CIRs).

Coronal Mass Ejections (CMEs) are massive eruptions of magnetized and ionized material from the solar

atmosphere, produced by a destabilization of the magnetic configuration at the corona. The interplanetary manifestation of CMEs (ICMEs) strongly distort the structure of the magnetic field and plasma conditions of the IP medium. One of the distinguishing ICMEs features is the presence of bi-directional streams of energetic (energy ~ 80 -1000 eV) electrons, parallel and/or antiparallel flows of suprathermal energy. This feature is generally viewed as a proxy of connectivity of the ICME's field lines to the Sun (e.g., Dasso et al., 2005a).

Because, generally, the eruption of CMEs is fast, the ejected material forms a shock wave while travelling towards the solar wind, accreting material ahead and forming a plasma sheath between the shock and the ejecta. When observed at 1 au, this is reflected in a typical ICME formed by sub-structures as shown in a superposed epoch constructed by using more than 40 well-behaved events (Masías-Meza et al., 2016).

Magnetic Clouds (MCs) are a sub-set of ICMEs, with specific observed properties (Burlaga et al., 1981): (1) it has an enhanced IMF with respect to the typical environment's solar wind, (2) it presents a smooth and large coherent rotation of the magnetic field vector to an *in situ* observer, and (3) it has a lower temperature than the expected for its bulk velocity (Démoulin, 2009).

This accumulated evidence indicates that MCs are formed by magnetic field lines forming a helical structure (a twisted flux tube called magnetic flux rope, or FR). Interplanetary FRs can be described locally using different MHD equilibrium 2D (symmetry of translation along a main axis) helical models. These models include a cylindrical geometry with different variants of circular force-free fields; oblate geometries such as elliptical or more complex shapes (with the major axis of the ellipse perpendicular to the Sun-Earth direction (e.g., Démoulin & Dasso, 2009b)); magneto static equilibria as Grad-Shafranov models (e.g., Möstl et al., 2009); etc.

The simplest and most used one is the circular linear force-free model (Lundquist, 1950), which is the theoretically expected MHD structure when relaxation is reached via dissipation of free energy keeping the magnetic helicity constant (i.e., the so-called MHD Taylor states). More details on different models to describe MCs can be found in the review of Dasso et al. (2005a) and references therein. The next step for describing IFRs allows the dynamical evolution of the FR, either considering simple analytical models (as quasi self-similar evolution (e.g., Démoulin & Dasso, 2009a)) or highly demanding MHD numerical simulations (e.g., Scolini et al., 2021).

It is believed that non-MC ICMEs correspond to a trajectory of the S/C passing near the canopy of the FR or to cases in which the FR was strongly distorted.

Figure 2 shows a cartoon of the main structures of the IP medium: the Parkerian solar wind, compression and rarefaction regions associated with SIRs/CIRs, and ICMEs/MCs. The figure shows that the feet of the flux rope inside MCs is attached/anchored to the solar surface. However, they can be attached or detached from the Sun. The magnetic configuration of ICMEs is very different from the typical Parkerian solar wind.

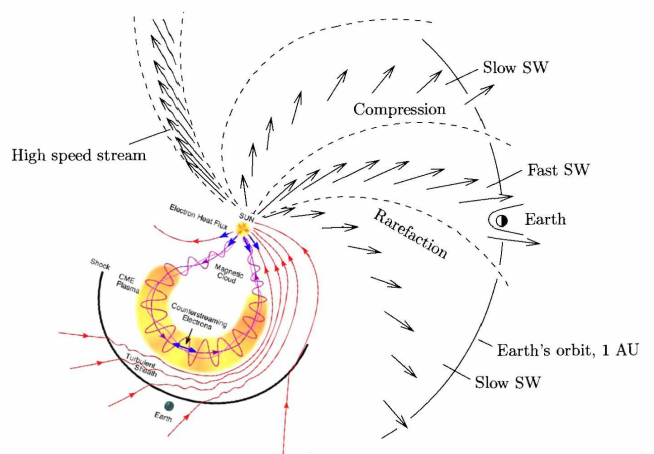


Figure 2: Cartoon showing examples of typical interplanetary structures as SIRs or ICMEs.

Also, interacting ICMEs can be found in the interplanetary medium (Dasso et al., 2009) due to a solar eruption produced after a previous one, with the second event ejected faster.

SIRs/CIRs and ICMEs/MCs are the interplanetary transients that produce the strongest disturbances to the geo-space, and also to the space environment of different planets (see e.g., Dasso et al., 2002, 2009; Molina et al., 2020).

In addition to providing knowledge about the Sun-Earth relation, *in situ* observations of ICMEs can improve our understanding of their solar origin. However, from their launching from the Sun, they evolve in the interplanetary medium under different physical processes that modify their size, magnetic structure and global shape. Furthermore, this evolution has an impact on our abilities to forecast, using remote solar observations, their impact when arriving at the Earth.

Several recent studies have statistically analyzed the evolution of ICMEs from *in situ* observations at different Ds (see, e.g., Gulisano et al., 2010, 2012; Janvier et al., 2019, and references therein).

ICMEs interact with their environment's solar wind during the journey from the Sun to the outer heliosphere and, since the solar wind total pressure (magnetic plus plasma) strongly decreases for increasing D , an ICME expansion is expected. The panel (a) in Figure 3 shows the increase in the ICME size (S) due to the decrease of the total solar wind environment's pressure.

When observed in a heliospheric frame by a spacecraft, the ICME's bulk plasma velocity typically decreases in magnitude from the front to its back, confirming the expectation that ICMEs are expanding. Furthermore, observations of large samples of events at different Ds , show that their size increases exponentially with D , such as $S/S_{ref} \sim (D/D_{ref})^\zeta$, where the sub-index ref indicates a reference value, for instance, near the Sun (e.g., Leitner et al., 2007; Gulisano et al., 2010, 2012).

From a theoretical base, Démoulin & Dasso (2009a) presented evidence about the fact that the physical origin of this expansion is due to the huge decrease in the interplanetary total pressure, which approximately fol-

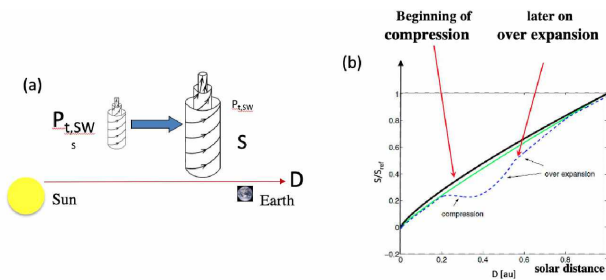


Figure 3: (a): Cartoon showing that, near the Sun, the total pressure is larger than near the Earth. Consequently, the size of the ICME is smaller near the Sun than near the Earth. (b): Figure showing two power laws (see main text) evolution of ICME size S (black and green lines). Evolution of S for a disturbed case (dashed blue line), when a local compression from 0.2 to 0.6 au is produced by a fast stream, then, the over-expansion adapts S to the environment's pressure when the interaction ends.

lows a power law of D : $P_{sw}/P_{sw,ref} \sim (D/D_{ref})^\gamma$, with $\gamma \sim 2.8$. From the conservation of the magnetic flux, a balance between the internal and external pressure, and assuming a quasi-stationary expansion and plasma beta near to zero inside ICMEs, these authors have shown a direct link between γ and ζ and a nearly self-similar evolution of the magnetic structure in the solar wind. In particular, for an isotropic expansion, they found the relationship between the solar wind total pressure decay and the ICME expansion rate as $\zeta = \gamma/4$. Thus, an expected value of $\zeta \sim 0.7$, which is consistent with different observations. Also, from a single case study of two radially aligned spacecraft (ACE at 1 au and Ulysses at ~ 5 au), Nakwacki et al. (2011) found that the observed value for ζ is fully consistent with observations at both heliodistances. However, for a certain limited time range during the travel from the Sun, some cases can expand at a different rate or even be in compression (Gulisano et al., 2010). The right panel (b) in Figure 3 shows a possible evolution of S vs. D for a local compression during the interaction of the ICME with another transient interplanetary structure, such as a fast stream from a coronal hole.

In situ observations provide plenty of information about the FR. This information can be split in scalar quantities and vector ones. For a correct analysis of the last ones, it is necessary to obtain a proper reference frame, and the one oriented as the FR main axis is the most convenient. The left panel in Figure 4 shows a scheme of the FR and the trajectory of the S/C crossing it (its trajectory can be approximated as a straight line because the velocity of the ICME is radial from the Sun and much larger than the velocity of the S/C, which can be approximated as at rest). The minimum distance between the trajectory of the S/C and the FR axis is frequently called ‘‘impact parameter’’ and it divides the observations within the FR into two branches: (1) the in-bound branch (red curve in Figure 4), which takes place when the S/C is entering into the FR, before reaching the minimum distance; and (2) the out-bound branch (blue curve in Figure 4), which happens when

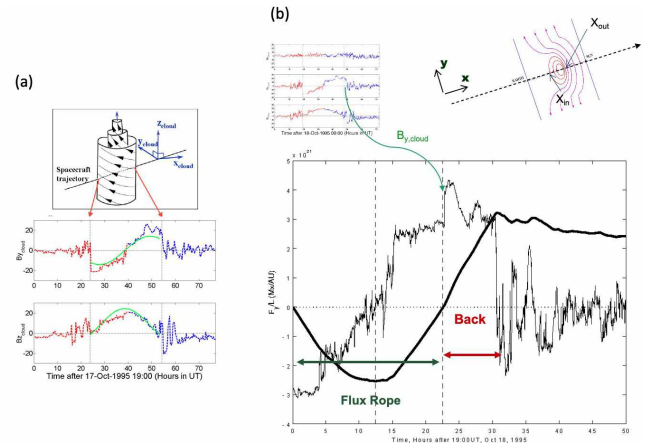


Figure 4: (a): Scheme showing the local system of reference oriented as the FR/cloud. (b): Example of consequences of erosion in a case studied, where a back is present after the closed magnetic structure finished.

the S/C is going out of the FR, after reaching the minimum distance from the FR axis.

Different methods have been used to estimate the FR orientation with *in situ* observations of the IMF. One of the most frequently used is the Minimum Variance method (see e.g., Gulisano et al., 2007; Démoulin et al., 2018, and references therein). The aging effects due to the expansion can pollute the accuracy of the methods to find the FR orientation. Démoulin et al. (2020) recently presented an algorithm to remove the aging effect and obtain the purely spatial magnetic shape of the FR, and, thus, to significantly improve the quality of the FR orientation.

From a case studied, after getting the components of the IMF in the local FR frame and the application of a technique for the computation of the magnetic flux in the two branches (in-bound and out-bound) of the FR, Dasso et al. (2006) found an extra flux in the out-bound branch, which is inconsistent with the presence of a magnetic FR, where the same flux in each branch is expected (for more details see Dasso et al. (2006, 2007)). This empirical result was interpreted as previous magnetic reconnection which produced erosion in the FR, producing its peeling and the presence of a back, see the right panel of Figure 4.

Later statistical studies have shown that the erosion process is present in a large number of FRs, sometimes producing peeling in the front and sometimes peeling the rear end of the FR (Ruffenach et al., 2015).

Numerical estimations from a case studied have shown that the intensity of a geomagnetic storm produced by a FR was reduced by $\sim 30\%$ due to FR erosion in comparison with a non-eroding FR (Lavraud et al., 2014). This shows that erosion during the travel of ICMEs from the Sun to Earth, can significantly affect the level of geoeffectiveness.

The twist distribution of the IMF field lines inside interplanetary FRs (i.e., number of turns per unit length) is under debate. This is determined by physical processes involved during its eruption from the Sun and by

the dynamical evolution during its interaction with the environment's solar wind. Because *in situ* IMF observations are carried out only along the S/C trajectory, it is necessary to complete observations with theoretical assumptions for modelling the twist. Furthermore, the IMF fluctuations that are present over the large scale IMF significantly increase the noise of the observed B time series and, thus, the bias of the deduced twist.

Recently, using a superposed epoch analysis of a significant sample of MCs, the typical twist distribution in MCs was determined (Lanabere et al., 2020a). It was found that the twist is nearly uniform near the FR core (approximately in the central half), but it increases moderately, up to a factor two, towards the MC outer part.

One of the most important MHD invariants associated with FRs is the magnetic helicity (H) (e.g., see the review Dasso, 2009). This quantity is crucially related with the twist distribution of IMF around the FR axis. One of the first statistical estimations of H in MCs was done by Dasso et al. (2006), where an inter-comparison between H in MCs in the IP medium and in their solar source region was done, finding a significant agreement. This study also validated the methods to compute H showing that, typically, the error bars and biases associated with different methods to model it are smaller than the variability of H for different events. Recently, Démoulin et al. (2016a) developed a statistical quantification of the total solar release of H , in a solar cycle, via erupting ICMEs.

The global shape of ICMEs can be tracked with imagers in the interplanetary space. However, they do not provide any direct estimation of the general FR properties.

Janvier et al. (2013, 2014, 2015) and Démoulin et al. (2016b) studied different aspects of ICMEs, using *in situ* observations, to constrain the global shape of shock wave and the flux rope axis from local measurements. They performed a statistical analysis of different sets of ICMEs including over more than 10 years of observations, analyzing the distribution of the angles that provide the local orientation of the FR axis and shock surface. A quantitative global shape of the sub-structures forming a typical ICME can be observed in Figure 11 of Démoulin et al. (2016b).

2.3. Interplanetary turbulence

Turbulence in the interplanetary medium has been studied developing theories and analyzing *in situ* observations from more than 60 years, finding several multi-scale space-time properties of the turbulence cascade, as it transfers energy from large scale reservoirs through the inertial range to the dissipation scales. A significant number of studies have been carried out using *in situ* single S/C observations, many of them analyzing them at 1 au (e.g., Dasso et al., 2005a), but also analyzing them at different distances from the Sun (e.g., Ruiz et al., 2011). However, all these single S/C studies need to assume the Taylor hypothesis, which allows the transference of the time domain into the space domain (Bruno & Carbone, 2013). Several recent works have analyzed turbulence

properties using simultaneous *in situ* observations at different points (i.e., purely spatial structures), taking advantage of the presence of S/Cs fleets (e.g., Matthaeus et al., 2005; Dasso et al., 2008; Weygand et al., 2009; Osman & Horbury, 2007), and even to decouple space-time from modelling the Eulerian decorrelation of fluctuations (Matthaeus et al., 2010). For more details on turbulence in the solar wind, see the live review of Bruno & Carbone (2013) and references therein.

Plasma macroscopic properties of ICMEs are different in comparison to the typical Parkerian solar wind. Some of them are key to determine the threshold of plasma instability for electromagnetic ion-cyclotron waves (EICWs). From theoretical studies, Dasso et al. (2003) have shown, for the first time, that the right-handed branch of EICWs is unstable in most ICMEs, driving free macroscopic energy to inject into MHD turbulence from different channels, than those found in the solar wind. Then, Matthaeus et al. (2008) found that some turbulent scales are significantly different in ICMEs, with respect to the Parkerian solar wind. This result confirms that turbulent activity in ICMEs is radically different. Other recent studies found significant differences in the waves and turbulent activity (e.g., Telsoni et al., 2020; Kilpua et al., 2020). Yet, there still is a significant amount of unanswered questions when it comes to the specific fluctuation properties in ICMEs.

3. Galactic Cosmic Rays

Galactic cosmic rays (GCRs) enter into the heliosphere from the local interstellar medium. They dominate the flux of energetic particles for a range of energy from \sim GeV to $\sim 10^5$ TeV and surround the heliosphere as a nearly constant and isotropic bath (e.g., Jokipii, 2010). The GCRs' flux decreases with energy roughly as a power law, varies with heliodistance D and has a different time variability (mainly due to the solar cycle, the presence of solar wind transients or changes in the turbulence level). The time variability of the GCRs' flux depends on the energy of the particle.

The transport of GCRs in the heliosphere is mainly governed by the combination of four major physical mechanisms: (a) Advection: the magnetized solar wind plasma, while escaping radially from the Sun at velocities of ~ 300 -700 km/s, advects cosmic rays. (b) Diffusion: An irregular motion of energetic particles due to the rugosity of the IMF. (c) Drifts: A large-scale variability of IMF produces coherent guiding-center drifts of GCRs, which is a basic problem of plasma physics (e.g., Jackson, 1998). And, finally, (d) Adiabatic changes on energy: Expansion/Compression of the parcels of fluid in the solar wind produces a decrease/increase of GCRs' energy, mainly due to changes on the separation of scatter centers. The master equation to describe these effects is known as "Parker's transport equation", after Eugene Parker who was the first one to write it (Parker, 1965).

As described in Sections 2.2 and 2.3, all the properties governing the flux of GCRs are significantly different inside ICMEs. Thus, it is expected that, during the passage of ICMEs near the Earth, cosmic rays

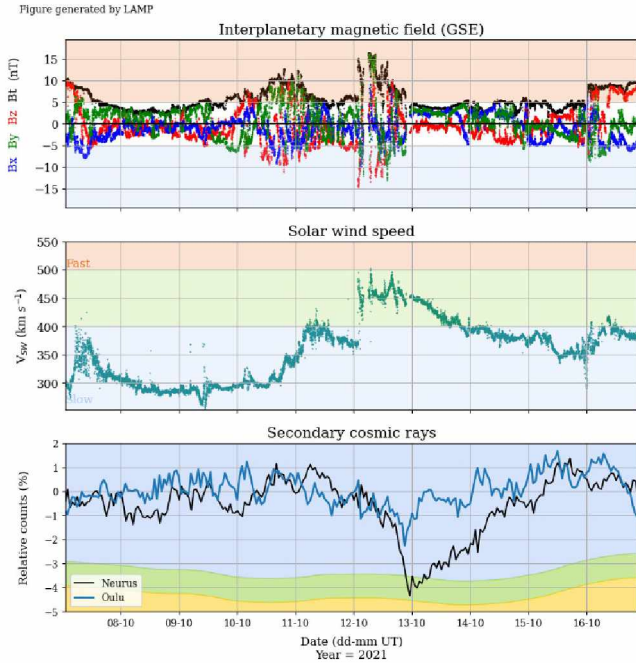


Figure 5: From *upper to bottom panels*: *in situ* observations of IMF at L1 (IP medium, near Earth): components (B_x, B_y and B_z in Geocentric Solar Ecliptic System, GSE) and modulus (B_t). Bulk plasma velocity. Relative variation of GCRs' flux, as observed by a NM (Oulu) and by Neurus. An ICME (*two upper panels*) and the consequent Forbush Decrease (*bottom panel*) are shown

ground observatories will detect flux variabilities. These decreases have been empirically well-known for several decades (e.g., Forbush, 1937; Cane, 2000), but the detailed causes determining the decrease in each substructure of the ICME are still under debate. Other solar wind transients that can produce decreases of GCRs' flux are SIRs (e.g., Gutierrez & Dasso, 2021)

4. The Argentine Space Weather Antarctic Laboratory

Neutron Monitors (NMs) have been the typical ground base instruments, used since the 1950s, to observe the variability of GCRs' fluxes (e.g., Meyer & Simpson, 1955). However, some years ago, other kinds of cosmic rays detectors started to be used for the analysis of IP effects on GCRs' fluxes. One of them is the Water Cherenkov Detector (WCD) (Pierre Auger Collaboration et al., 2011; Dasso et al., 2012; Asorey et al., 2015). Due to the geomagnetic shielding, several NMs are located in Antarctica, obtaining the most important observations.

Almost a decade ago, our LAMP group in the framework of the Space Weather program of the Latin American Giant Observatory (LAGO) collaboration, which is an extended observatory of cosmic rays using WCDs (www.lagoproject.net) and is a spin-off of the Pierre Auger Observatory, developed a project and carried out different studies of the site to install a LAGO node at

the Argentine Marambio base in Antarctica, located at 64S/56W and 200 meters asl (see, e.g., Dasso et al., 2015).

A detector (called *Neurus*) was built by LAMP in the space laboratory of IAFE (Institute of Astronomy and Astrophysics, UBA-CONICET), with improvements in comparison with the typical detectors of LAGO, to adapt it to the extreme conditions in Antarctica, which can reach temperatures of -40 Celsius degrees and winds of 300 km/h. Some partial advances of the construction and calibration of *Neurus* were published by advanced students that worked on different tasks (e.g., Coppola et al., 2016).

The project was finally extended and, in the summer campaign of 2018-2019, LAMP deployed its own full Space Weather laboratory at Marambio, where several space weather instruments, besides *Neurus* (that is the Antarctic node of LAGO) are hosted. For the deployment, more than three tons of scientific cargo were taken to Antarctica. An in-house meteorological station (also adapted to extreme conditions), calibrated at the SMN (*Servicio Meteorológico Nacional of Argentina*), was also installed to calibrate the cosmic rays data. The accuracy of the time stamp for the data is guaranteed using a GPS system in a pps mode. The full system has redundancy, and the telemetry from Antarctica to our servers in Buenos Aires uses satellite internet signal, with a delay of only 5 minutes. More details on the current state of the laboratory can be found in Gulisano et al. (2021).

Preliminary results of *Neurus* were published by Santos et al. (2021). They show the validation of the detector from comparisons with NMs. Also, a paper that shows *Neurus*'s capability to measure spatial anisotropy of the GCRs' flux was recently submitted (Santos et al., 2022).

Figure 5 shows, from the upper to the bottom panels, the observed IMF (modulus and components in GSE), the solar wind bulk velocity and the variability of the flux of GCRs observed by two detectors: a NM at Oulu and *Neurus* WCD at Marambio. From the analysis of this figure we can observe the presence of an ICME, on October 12th, with high values of the IMF, a jump in the solar wind speed (a shock preceding the ejecta), and a consequent Forbush decrease that reaches $\sim -2\%$ at Oulu and $\sim -4\%$ at Marambio, with the peak observed at the same time with both detectors.

This kind of figures with real time data on solar wind near the Earth and variations of GCRs' flux from *Neurus* can be found at the web site of the LAMP group: spaceweather.at.fcen.uba.ar (Lanabere et al., 2021).

5. Summary and Conclusions

The heliosphere is a physical scenario presenting a variety of physical processes which are also present in other astrophysical systems. The direct access to *in situ* observations makes it an ideal system to test theories and to improve the modelling of astrophysical processes such as magnetic reconnection, MHD turbulence, transport of energetic particles in astrophysical plasmas, etc.

In this review paper, I presented a brief summary of solar wind properties emphasizing on ICMEs, which are the most geo-effective interplanetary events and are the major cause of GCRs' fluxes decrease near the Earth. A recent LAMP Space Weather laboratory, the first one in an Argentine Antarctic base (Marambio), which is operating since 2019, was also briefly described. In this laboratory, among other instruments, a Water Cherenkov detector called *Neurus* (also a node of LAGO) measures the flux of GCRs, for both basic and fundamental scientific purposes and also for real-time monitoring.

The huge amount of results obtained during the last years have paved the way for significant advances on the knowledge of IP properties and effects on GCRs' transport. However, some key questions are still waiting to be unveiled, mainly, using new fleets of spacecrafts and modern highly demanding numerical simulations.

Acknowledgements: SD acknowledges support from the Argentinean grants: PICT-2019-02754 (FONCyT-ANPCyT) and UBACyT-20020190100247BA (UBA).

References

- Asorey H., et al., 2015, Proc. Sci., ICRC2015, PoS(ICRC2015)142
- Baker D.N., et al., 2013, Space Weather, 11, 585
- Bruno R., Carbone V., 2013, Living Rev. Sol. Phys., 10
- Burlaga L., et al., 1981, J. Geophys. Res., 86, 6673
- Cane H.V., 2000, SSRv, 93, 55
- Coppola M., et al., 2016, BAAA, 58, 278
- Daglis I.A., et al., 2021, Annales Geophysicae, 39, 1013
- Dasso S., 2009, N. Gopalswamy, D.F. Webb (Eds.), *Universal Heliophysical Processes*, vol. 257, 379–389
- Dasso S., Asorey H., Pierre Auger Collaboration, 2012, Adv. Space Res., 49, 1563
- Dasso S., Gómez D., Mandrini C.H., 2002, J. Geophys. Res. Space Phys., 107, 1059
- Dasso S., Gratton F.T., Farrugia C.J., 2003, J. Geophys. Res., 108, 1149
- Dasso S., et al., 2005a, ApJ, 635, L181
- Dasso S., et al., 2005b, Adv. Space Res., 35, 711
- Dasso S., et al., 2006, A&A, 455, 349
- Dasso S., et al., 2007, Solar Phys., 244, 115
- Dasso S., et al., 2008, *International Cosmic Ray Conference, International Cosmic Ray Conference*, vol. 1, 625–628
- Dasso S., et al., 2009, J. Geophys. Res. Space Phys., 114, A02109
- Dasso S., et al., 2015, *Proceedings of Science, PoS(ICRC2015)105*, The Hague
- Démoulin P., 2009, Solar Phys., 257, 169
- Démoulin P., Dasso S., 2009a, A&A, 498, 551
- Démoulin P., Dasso S., 2009b, A&A, 507, 969
- Démoulin P., Dasso S., Janvier M., 2018, A&A, 619, A139
- Démoulin P., Janvier M., Dasso S., 2016a, Solar Phys., 291, 531
- Démoulin P., et al., 2016b, A&A, 595, A19
- Démoulin P., et al., 2020, A&A, 639, A6
- Dorsch B.D., Spago S.C., Santos N. A. Dasso S., 2022, BAAA, "submitted"
- Forbush S.E., 1937, Phys. Rev., 51, 1108
- Gulisano A.M., et al., 2007, Adv. Space Res., 40, 1881
- Gulisano A.M., et al., 2010, A&A, 509, A39
- Gulisano A.M., et al., 2012, A&A, 543, A107
- Gulisano A.M., et al., 2021, BAAA, 62, 280
- Gutierrez C., Dasso S., 2021, BAAA, 62, 13
- Hapgood M., Huixin L., Lugaz N., 2022, Space Weather, 11, 585
- Hayakawa H., et al., 2019, MNRAS, 484, 4083
- Jackson J.D., 1998, *Classical Electrodynamics, 3rd Edition*
- Janvier M., Démoulin P., Dasso S., 2013, A&A, 556, A50
- Janvier M., Démoulin P., Dasso S., 2014, A&A, 565, A99
- Janvier M., et al., 2015, J. Geophys. Res. Space Phys., 120, 3328
- Janvier M., et al., 2019, J. Geophys. Res. Space Phys., 124, 812
- Jokipii J.R., 2010, C.J. Schrijver, G.L. Siscoe (Eds.), *Heliophysics: Evolving Solar Activity and the Climates of Space and Earth*, 243–268
- Kilpua E.K.J., et al., 2020, Annales Geophysicae, 38, 999
- Lanabere V., et al., 2020a, A&A, 635, A85
- Lanabere V., et al., 2020b, Adv. Space Res., 65, 2223
- Lanabere V., et al., 2021, BAAA, 62, 4
- Lavraud B., et al., 2014, J. Geophys. Res. Space Phys., 119, 26
- Leitner M., et al., 2007, J. Geophys. Res. Space Phys., 112, A06113
- Lundquist S., 1950, *Ark. Fys.*, 2, 361
- Masias-Meza J.J., et al., 2016, A&A, 592, A118
- Matthaeus W.H., et al., 2005, Phys. Rev. Lett., 95, 231101
- Matthaeus W.H., et al., 2008, ApJL, 678, L141
- Matthaeus W.H., et al., 2010, ApJL, 721, L10
- Meyer P., Simpson J.A., 1955, Phys. Rev., 99, 1517
- Molina M.G., et al., 2020, Solar Phys., 295, 173
- Möstl C., et al., 2009, Solar Phys., 256, 427
- Nakwacki M.S., et al., 2011, A&A, 535, A52
- Osman K.T., Horbury T.S., 2007, ApJ, 654, L103
- Parker E.N., 1965, Planet. Space Sci., 13, 9
- Pierre Auger Collaboration, et al., 2011, J. Instrum., 6, 1003
- Ruffenach A., et al., 2015, J. Geophys. Res. Space Phys., 120, 43
- Ruiz M.E., et al., 2011, J. Geophys. Res., 116, A10102
- Russell C.T., Luhmann J.G., Strangeway R.J., 2016, *Space Physics - An Introduction*, 1st ed. ed., Cambridge Univ. Press, New York, NY
- Santos N.A., et al., 2021, BAAA, 62, 16
- Santos N.A., et al., 2022, Solar Phys., "submitted",
- Scolini C., et al., 2021, A&A, 649, A69
- Telloni D., et al., 2020, ApJL, 905, L12
- Weygand J.M., et al., 2009, J. Geophys. Res. Space Phys., 114, A07213